

Global asymptotic stability of an active disassembly model of flagellar length control

Thomas G. Fai^{*,†} and Youngmin Park^{*}

^{*}Department of Mathematics, Brandeis University, Waltham, Massachusetts 02453

[†]Volen Center for Complex Systems, Brandeis University, Waltham, Massachusetts 02453

Abstract

Organelle size control is a fundamental question in biology that demonstrates the fascinating ability of cells to maintain homeostasis within their highly variable environments. Theoretical models describing cellular dynamics have the potential to help elucidate the principles underlying size control. Here, we perform a detailed mathematical study of the active disassembly model proposed in [Fai et al, Length regulation of multiple flagella that self-assemble from a shared pool of components, *eLife*, 8, (2019): e42599]. We construct a Lyapunov function to show that the dynamical equations for the flagellar lengths are well-behaved and rule out the possibility of oscillations in the model. We prove global asymptotic stability in the case of two flagella and show that this result generalizes to arbitrary flagellar number. Our analysis reveals a defect in the original active disassembly model, which is manifested as corners in the phase space that yield unphysical solutions. To address this defect, we construct a hybrid system. Although this hybrid system leads to behaviors such as time delays and the accumulation of trajectories in the corners of phase space, we show that these scenarios do not typically arise in applications.

Key words: length control; flagella; mathematical modeling; dynamical systems

Robust size control is essential in biology at the levels of organs, cells, and organelles. The absence of size regulation is a marker of pathologies such as cancer [1], and the varied sizes of biological structures highlight differences in the fundamental physical constraints on biological systems [2, 3, 4].

At the level of organelles, a particular useful model organism for flagellar length control is the unicellular green algae *Chlamydomonas reinhardtii* (Figure 1(a))[5, 6, 7, 8, 9]. *Chlamydomonas* uses its two flagella to propel itself through its aqueous environment and the lengths of its flagella are important for maintaining swimming speed and direction [10, 11].

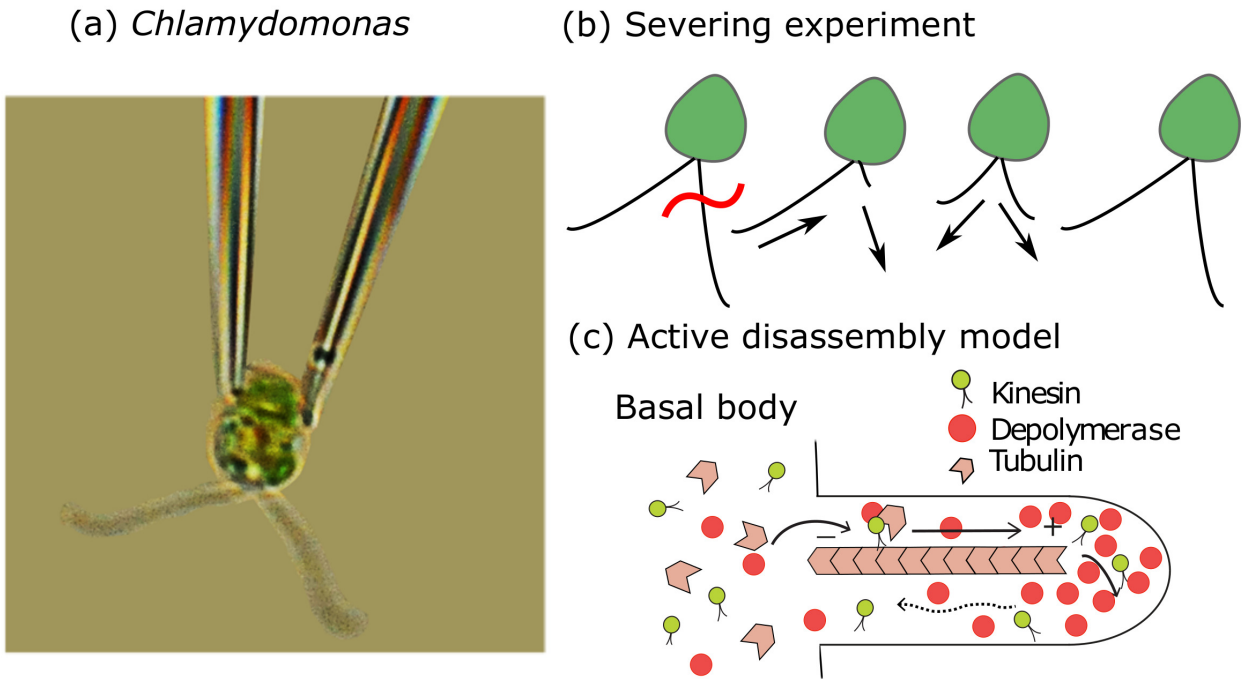


Figure 1: *Chlamydomonas reinhardtii* and the active disassembly model of flagellar length control. (a) Experimental image of *Chlamydomonas* from [7] provided by the author. The two flagella have equal lengths of approximately 12 μm . (b) Upon severing one flagellum, the severed flagellum begins to regenerate while the unsevered flagellum shortens. The flagella rapidly equalize at an intermediate length before returning to their initial lengths on a slower timescale. (c) Schematic of the active disassembly model [13], in which the concentration gradient generated by a diffusing depolymerase leads to a length-dependent rate of disassembly at the flagellar tip.

Experiments on *Chlamydomonas* show that flagellar maintenance and length control is a dynamic process. During severing experiments in which a single flagellum is amputated, there is an initial phase in which the two flagellar lengths equalize to a shorter intermediate length and a subsequent phase in which the two flagella grow together to the initial steady-state length [12] (shown schematically in Figure 1(b)). This reveals the coupling between the length dynamics of the two flagella.

The balance-point model, in which the steady-state length is determined by the competition between assembly and disassembly processes, has been proposed to account for the length regulation observed in severing experiments [14, 15]. Here, we focus on a particular balance point model suitable for organisms such as *Chlamydomonas reinhardtii*, in which multiple flagella are assembled simultaneously from a shared pool of building blocks. In the original balance-point model proposed for *Chlamydomonas*, the assembly rate is taken to be a monotonically decreasing function of length whereas the disassembly rate

is taken to be length-independent [14, 15]. This yields a unique point of intersection that determines the steady-state length.

We have shown previously [13] that it is important to consider not only the predictions of the balance-point model for a single flagellum, but also its predictions for the coupled behavior of two (or more) flagella in light of severing experiments. Whereas constant disassembly models are unable to account for the length-equalization observed in severing experiments, we have proposed an active disassembly model based on physical first principles of flux balance (Figure 1(c)) in which length-dependent disassembly leads to simultaneous length control.

In this work, we consider the mathematical properties of the active disassembly model as a system of nonlinear ordinary differential equations. We show that these equations have a global asymptotically stable steady-state solution. To prove this, we find a Lyapunov function for the dynamics. The Lyapunov function also implies there are no limit cycles or periodic oscillations. However, there is still the possibility of nontrivial dynamics. We construct a hybrid system to ensure that the flagellar lengths remain non-negative, and this yields regions of state space from which all trajectories contract to a single point on the boundary before flowing toward steady-state. We interpret these trajectories in light of existing experimental data. In addition, we provide alternate proofs of global asymptotic stability and the non-existence of periodic oscillations that do not rely on the construction of a Lyapunov function. We discuss how these results generalize to other situations.

By characterizing the mathematical properties of the active disassembly model, we aim to provide a strong foundation for subsequent applications and analysis of the model. In the Discussion, we note several open questions regarding the mathematical model and its application to flagellar length control in *Chlamydomonas*.

1 Active disassembly model of flagellar length control

Flagella are dynamic structures. During the process known as intraflagellar transport (IFT), protein assemblies known as IFT trains are transported by motor molecules, some that carry trains toward the tip (anterograde direction) and others that carry IFT trains toward the base of the flagella (retrograde direction) [16]. In the balance-point model, this turnover is captured by the continual assembly and disassembly processes which reach a dynamic steady-state.

Let $L_1(t)$ and $L_2(t)$ denote the lengths of two flagella on a single *Chlamydomonas* organism at a particular time t . The flagellum is composed of tubulin filaments, and we assume there is a total amount T of tubulin available.

Similarly, we assume there are a total number M of anterograde molecular motors, of which a number M_f are present in the pool at the flagellar base while the rest are undergoing IFT. The motors move ballistically in the anterograde direction with velocity and diffusively in the retrograde direction with diffusion coefficient D [17]. The injection

flux J of IFT particles into the flagella satisfies mass action kinetics, so that

$$J = k_{\text{on}}M_f. \quad (1)$$

There is a separation of timescales between the motion of IFT particles, which traverse the flagellum in several seconds, and the flagellar length dynamics, which varies over a timescale of several minutes [18]. As shown in [13], upon combining (1) with conservation of protein number, this separation of timescales leads to a quasi-steady state approximation for the flux:

$$J = \frac{k_{\text{on}}M/2}{1 + k_{\text{on}}(L_1 + L_2)/2v + k_{\text{on}}(L_1^2 + L_2^2)/4D}. \quad (2)$$

The flux J represents the number of IFT particles injected per second into the flagella, and these trains are assumed to carry an amount of tubulin proportional to the free tubulin in the basal pool. Therefore, the overall speed of assembly is equal to:

$$\text{assembly} = \gamma J (T - L_1 - L_2), \quad (3)$$

where γ is a proportionality constant that represents the fraction of tubulin arriving at the flagellar tip that is incorporated into the flagellum. Disassembly is taken to be a linear function of the depolymerase concentration at the flagellar tip, i.e. each depolymerizing enzyme located near the flagellar tip removes a constant number of tubulin subunits per second. This implies that for the i^{th} flagellum, the speed of disassembly satisfies

$$\text{disassembly}_i = d_0 + d_1 \frac{JL_i}{D}, \quad (4)$$

for $i = 1, 2$, assuming that the depolymerase has the same pattern of motion as the anterograde motors [13]. Setting the growth rate to be the difference between assembly and disassembly speeds leads to a system of coupled nonlinear differential equations:

$$L_1' = \gamma J (T - L_1 - L_2) - d_0 - d_1 \frac{JL_1}{D} \quad (5)$$

$$L_2' = \gamma J (T - L_1 - L_2) - d_0 - d_1 \frac{JL_2}{D}. \quad (6)$$

where $J \equiv J(L_1, L_2)$ satisfies

$$J(L_1, L_2) = \frac{k_{\text{on}}M/2}{1 + k_{\text{on}}(L_1 + L_2)/2v + k_{\text{on}}(L_1^2 + L_2^2)/4D}. \quad (7)$$

1.1 Nondimensionalization

We next rewrite (5) and (6) in dimensionless form. In terms of the nondimensional length $\tilde{L} = L/T$ and nondimensional time $\tilde{t} = t\gamma k_{\text{on}}M/2$ as well as the dimensionless parameters

$\pi_0 = 2d_0/\gamma k_{\text{on}}MT$, $\pi_1 = d_1/\gamma D$, $\pi_2 = k_{\text{on}}T/2v$, and $\pi_3 = k_{\text{on}}T^2/4D$, the system of equations (5) and (6) becomes

$$\frac{d\tilde{L}_1}{d\tilde{t}} = \tilde{J} \left(1 - \tilde{L}_1 - \tilde{L}_2\right) - \pi_0 - \pi_1 \tilde{J} \tilde{L}_1 \quad (8)$$

$$\frac{d\tilde{L}_2}{d\tilde{t}} = \tilde{J} \left(1 - \tilde{L}_1 - \tilde{L}_2\right) - \pi_0 - \pi_1 \tilde{J} \tilde{L}_2, \quad (9)$$

where the dimensionless flux $\tilde{J} = 2J/k_{\text{on}}M$ satisfies

$$\tilde{J} = \frac{1}{1 + \pi_2(\tilde{L}_1 + \tilde{L}_2) + \pi_3(\tilde{L}_1^2 + \tilde{L}_2^2)}. \quad (10)$$

We interpret the dimensionless parameters as follows: π_0 is the ratio of disassembly and assembly rates, π_1 is the depolymerase activity level, $\pi_2 = \tau_b/\tau_i$ is the ratio of the ballistic timescale $\tau_b := T/v$ of IFT transport to the injection timescale $\tau_i := k_{\text{on}}^{-1}$, and $\pi_3 = \tau_d/\tau_i$ is an analogous ratio of the diffusive timescale $\tau_d = T^2/2D$ to the injection timescale. (We could equivalently think of π_2 and π_3 as ratios of lengthscales related to the same physical processes.)

It is a straightforward calculation to verify that both flagella have the same steady-state length \tilde{L}_{ss} given by

$$\tilde{L}_{\text{ss}} = \frac{1 + \pi_0\pi_2 + \pi_1/2}{2\pi_0\pi_3} \left(\sqrt{1 + \frac{2(1 - \pi_0)\pi_0\pi_3}{(1 + \pi_0\pi_2 + \pi_1/2)^2}} - 1 \right). \quad (11)$$

2 Nonlinear behavior

To simplify notation, we drop tildes and use the dimensionless formulation for the remainder of the article. The active disassembly model (8) and (9) is not a gradient system, i.e. it cannot be written as the gradient of an energy function $E(L_1, L_2)$. This is proven by contradiction. Suppose there is an energy function such that $L'_1 = \partial E/\partial L_1$ and $L'_2 = \partial E/\partial L_2$. Then, by equality of mixed partials

$$\frac{\partial^2 E}{\partial L_1 \partial L_2} = \frac{\partial L'_1}{\partial L_2} = \frac{\partial L'_2}{\partial L_1} = \frac{\partial^2 E}{\partial L_2 \partial L_1}, \quad (12)$$

i.e.

$$\frac{\partial (J(1 - L_1 - L_2) - \pi_0 - \pi_1 J L_1)}{\partial L_2} = \frac{\partial (J(1 - L_1 - L_2) - \pi_0 - \pi_1 J L_2)}{\partial L_1}. \quad (13)$$

However, the left-hand side of the the inequality is equal to

$$-J + (1 - L_1 - L_2) \frac{\partial J}{\partial L_2} - \pi_1 L_1 \frac{\partial J}{\partial L_2}, \quad (14)$$

whereas the right-hand side is equal to

$$-J + (1 - L_1 - L_2) \frac{\partial J}{\partial L_1} - \pi_1 L_2 \frac{\partial J}{\partial L_1}. \quad (15)$$

Because $J(L_1, L_2) = J(L_2, L_1)$, we have $\partial J / \partial L_1 = \partial J / \partial L_2$. Assuming $\pi_1 \neq 0$, follows that there is equality if and only if $L_1 = L_2$. We have thereby reached the contradiction since $L_1 \neq L_2$ in general. It follows that no energy function exists.

However, using a technique applicable to many nonlinear dynamical systems, we may construct a Lyapunov function to show that the steady state is globally asymptotically stable. First, we specify the subspace Ω with $(L_1, L_2) \in \Omega \subset \mathbb{R}^2$ over which the model is defined. Because we must have $L_1, L_2 \geq 0$ for the variables to have physical meaning as lengths, Ω is contained within the first quadrant. Moreover, the sum of lengths cannot exceed the total pool size so that $L_1 + L_2 \leq 1$. To summarize, Ω is defined to be the triangular region in the first quadrant bound by the lines $L_1 = 0$, $L_2 = 0$, and $L_1 + L_2 \leq 1$.

We define the deviations from steady-state $\Delta L_1 := L_1 - L_{ss}$ and $\Delta L_2 := L_2 - L_{ss}$ on Ω and express the dynamics in terms of ΔL_1 and ΔL_2 :

$$\frac{dL_1}{dt} = J(1 - 2L_{ss} - \Delta L_1 - \Delta L_2) - \pi_0 - \pi_1 J(L_{ss} + \Delta L_1) \quad (16)$$

$$\frac{dL_2}{dt} = J(1 - 2L_{ss} - \Delta L_1 - \Delta L_2) - \pi_0 - \pi_1 J(L_{ss} + \Delta L_2), \quad (17)$$

or equivalently

$$\frac{dL_1}{dt} = J(1 - 2L_{ss}) - J(\Delta L_1 + \Delta L_2) - \pi_0 - \pi_1 J L_{ss} - \pi_1 J \Delta L_1 \quad (18)$$

$$\frac{dL_2}{dt} = J(1 - 2L_{ss}) - J(\Delta L_1 + \Delta L_2) - \pi_0 - \pi_1 J L_{ss} - \pi_1 J \Delta L_2. \quad (19)$$

By symmetry, the steady-state lengths $L_{1,ss}$ and $L_{2,ss}$ are equal. We denote the common steady-state length by L_{ss} . It is determined by setting the derivative equal to zero in (18) or (19), which yields the identity

$$0 = J_{ss}(1 - 2L_{ss}) - \pi_0 - \pi_1 J_{ss} L_{ss}, \quad (20)$$

where

$$J_{ss} = \frac{1}{1 + 2\pi_2 L_{ss} + 2\pi_3 L_{ss}^2}. \quad (21)$$

(Eq. (20) yields a quadratic equation for L_{ss} , which has a unique positive root given by (11).)

We next use the steady-state relationship (20) to rewrite (18) and (19) in a different form. Before we proceed, we first note the identities given by

$$J(1 - 2L_{ss}) = (J - J_{ss})(1 - 2L_{ss}) + J_{ss}(1 - 2L_{ss}) \quad (22)$$

$$\pi_1 J L_{ss} = \pi_1 (J - J_{ss}) L_{ss} + \pi_1 J_{ss} L_{ss}, \quad (23)$$

where the first line follows from adding and subtracting $J_{ss}(1 - 2L_{ss})$ and the second line follows from adding and subtracting $\pi_1 J_{ss} L_{ss}$. Plugging the above expressions into (18) and (19) and using the steady-state relation (20) yields

$$\frac{dL_1}{dt} = (J - J_{ss})(1 - 2L_{ss}) - J(\Delta L_1 + \Delta L_2) - \pi_1(J - J_{ss})L_{ss} - \pi_1 J \Delta L_1 \quad (24)$$

$$\frac{dL_2}{dt} = (J - J_{ss})(1 - 2L_{ss}) - J(\Delta L_1 + \Delta L_2) - \pi_1(J - J_{ss})L_{ss} - \pi_1 J \Delta L_2. \quad (25)$$

Adding and subtracting the above equations yields

$$\frac{dL_1}{dt} + \frac{dL_2}{dt} = 2(J - J_{ss})(1 - 2L_{ss} - \pi_1 L_{ss}) - (2 + \pi_1)J(\Delta L_1 + \Delta L_2) \quad (26)$$

$$\frac{dL_1}{dt} - \frac{dL_2}{dt} = -\pi_1 J(\Delta L_1 - \Delta L_2) \quad (27)$$

It follows that

$$\frac{1}{2} \frac{d}{dt} (\Delta L_1 + \Delta L_2)^2 = 2(J - J_{ss})(1 - 2L_{ss} - \pi_1 L_{ss})(\Delta L_1 + \Delta L_2) - (2 + \pi_1)J(\Delta L_1 + \Delta L_2)^2 \quad (28)$$

$$\frac{1}{2} \frac{d}{dt} (\Delta L_1 - \Delta L_2)^2 = -\pi_1 J(\Delta L_1 - \Delta L_2)^2. \quad (29)$$

where we have used $dL_i/dt = d(L_{ss} + \Delta L_i)/dt = d\Delta L_i/dt$ for $i = 1, 2$ and

$$\frac{1}{2} \frac{d(\Delta L_1 + \Delta L_2)^2}{dt} = (\Delta L_1 + \Delta L_2) \frac{d(\Delta L_1 + \Delta L_2)}{dt} \quad (30)$$

$$\frac{1}{2} \frac{d(\Delta L_1 - \Delta L_2)^2}{dt} = (\Delta L_1 - \Delta L_2) \frac{d(\Delta L_1 - \Delta L_2)}{dt}. \quad (31)$$

We use (28) and (29) to form a Lyapunov function for the dynamics. Let

$$\phi(L_1, L_2) = \frac{1}{2} \left[(\Delta L_1 + \Delta L_2)^2 + \frac{\pi_3}{\pi_1} (\Delta L_1 - \Delta L_2)^2 \right]. \quad (32)$$

Claim. ϕ is a Lyapunov function on Ω .

We first comment on some implications of the above claim before proceeding with its proof. It follows from the claim that there is a unique steady-state L_{ss} at which $(L_1, L_2) = (L_{ss}, L_{ss}) \in \Omega$ and that no limit cycles exist in Ω .

Proof. Since it is the sum of squared terms with positive factors, $\phi \geq 0$. It remains to show that $\phi' \leq 0$ with equality achieved only at the unique steady-state $L_1 = L_2 = L_{ss}$. Because the second term of ϕ has a non-positive derivative (by (29)), a sufficient condition for $\phi' \leq 0$ is that the right-hand side of (28) is negative away from the steady-state, i.e.

$$2(J - J_{ss})(1 - 2L_{ss} - \pi_1 L_{ss})(\Delta L_1 + \Delta L_2) - (2 + \pi_1)J(\Delta L_1 + \Delta L_2)^2 < 0, \quad (33)$$

except when $\Delta L_1 = \Delta L_2 = 0$ in which case it is zero. As we show next, in some cases (33) holds and the claim immediately follows. Later on, we show how, if (33) does not hold, we may use the second term of ϕ to obtain the desired result $\phi' \leq 0$.

It follows from the steady-state condition (20) that

$$1 - 2L_{ss} - \pi_1 L_{ss} = \frac{\pi_0}{J_{ss}}. \quad (34)$$

Therefore, the first term on the left-hand side of (33) may be rewritten as

$$\begin{aligned} 2(J - J_{ss})(1 - 2L_{ss} - \pi_1 L_{ss})(\Delta L_1 + \Delta L_2) &= \frac{2\pi_0}{J_{ss}}(J - J_{ss})(\Delta L_1 + \Delta L_2) \\ &= 2\pi_0 J_{ss}^{-1} \left(\frac{1}{J^{-1}} - \frac{1}{J_{ss}^{-1}} \right) (\Delta L_1 + \Delta L_2) \\ &= 2\pi_0 J_{ss}^{-1} \left(\frac{J_{ss}^{-1} - J^{-1}}{J_{ss}^{-1} J^{-1}} \right) (\Delta L_1 + \Delta L_2) \\ &= 2\pi_0 J \left(J_{ss}^{-1} - J^{-1} \right) (\Delta L_1 + \Delta L_2). \end{aligned} \quad (35)$$

To simplify the right-hand side of the above expression, we use the definition of the flux (10) to get

$$\begin{aligned} J_{ss}^{-1} - J^{-1} &= 1 + 2\pi_2 L_{ss} + 2\pi_3 L_{ss}^2 - \left(1 + \pi_2 (L_1 + L_2) + \pi_3 (L_1^2 + L_2^2) \right) \\ &= -\pi_2 (\Delta L_1 + \Delta L_2) - \pi_3 (L_{ss}^2 - L_1^2 + L_{ss}^2 - L_2^2). \end{aligned} \quad (36)$$

Note that

$$\begin{aligned} L_1^2 - L_{ss}^2 + L_2^2 - L_{ss}^2 &= (L_1 + L_{ss})\Delta L_1 + (L_2 + L_{ss})\Delta L_2 \\ &= L_1 \Delta L_1 + L_2 \Delta L_2 + L_{ss}(\Delta L_1 + \Delta L_2), \end{aligned} \quad (37)$$

and moreover

$$\begin{aligned} L_1 \Delta L_1 + L_2 \Delta L_2 &= \frac{L_1 + L_2}{2} (\Delta L_1 + \Delta L_2) + \left(L_1 - \frac{L_1 + L_2}{2} \right) \Delta L_1 + \left(L_2 - \frac{L_1 + L_2}{2} \right) \Delta L_2 \\ &= \frac{L_1 + L_2}{2} (\Delta L_1 + \Delta L_2) + \frac{L_1 - L_2}{2} \Delta L_1 - \frac{L_1 - L_2}{2} \Delta L_2 \\ &= \frac{L_1 + L_2}{2} (\Delta L_1 + \Delta L_2) + \frac{1}{2} (\Delta L_1 - \Delta L_2)^2. \end{aligned} \quad (38)$$

Combining (35) to (38), for the left-hand side of (33) we have

$$\begin{aligned} 2\pi_0 J \left(J_{ss}^{-1} - J^{-1} \right) (\Delta L_1 + \Delta L_2) &= -2\pi_0 J \left(\pi_2 (\Delta L_1 + \Delta L_2)^2 + \pi_3 L_{ss} (\Delta L_1 + \Delta L_2)^2 \right. \\ &\quad \left. + \frac{\pi_3}{2} (L_1 + L_2) (\Delta L_1 + \Delta L_2)^2 + \frac{\pi_3}{2} (\Delta L_1 - \Delta L_2)^2 (\Delta L_1 + \Delta L_2) \right). \end{aligned} \quad (39)$$

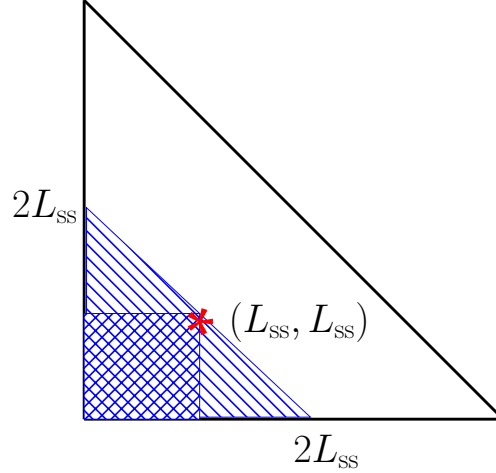


Figure 2: Schematic of the triangular region Ω^t used in the proof. Ω^t is illustrated by the diagonal pattern; it is defined as the region in which $\Delta L_1 + \Delta L_2 < 0$. The subset of Ω^t in which both $\Delta L_1 < 0$ and $\Delta L_2 < 0$ is illustrated by the crosshatched pattern.

To show the above expression is negative, we consider two cases. In the case $\Delta L_1 + \Delta L_2 > 0$, the term in parentheses on the right-hand side of (39) is a sum of squared terms multiplied by positive numbers. Therefore the right-hand side of (39) is negative.

In the case $\Delta L_1 + \Delta L_2 < 0$, we may bound the positive term by the negative terms in the right-hand side of (39) to show that the overall expression is negative. In this case, (L_1, L_2) must reside in a triangular subset $\Omega^t \subset \Omega$ (the striped region in Fig. 2). On this subset, if both ΔL_1 and ΔL_2 are negative, then

$$|\Delta L_1 - \Delta L_2| < |\Delta L_1 + \Delta L_2|, \quad (40)$$

and moreover $|\Delta L_1 - \Delta L_2| < |\Delta L_1| + |\Delta L_2| < 2L_{ss}$, so that

$$\frac{\pi_3}{2} |\Delta L_1 - \Delta L_2|^2 |\Delta L_1 + \Delta L_2| \leq \pi_3 L_{ss} |\Delta L_1 + \Delta L_2|^2, \quad (41)$$

and since this term already appears in (39) with a minus sign it follows that the right-hand side of (39) is negative.

On the other hand, if ΔL_1 and ΔL_2 have opposite signs, then we must use a different bound. From the geometry of the relevant triangular subset $\Omega^t \subset \Omega$, we have as before $|\Delta L_1 + \Delta L_2| \leq 2L_{ss}$ so that

$$\frac{\pi_3}{2} |\Delta L_1 - \Delta L_2|^2 |\Delta L_1 + \Delta L_2| \leq \pi_3 L_{ss} |\Delta L_1 - \Delta L_2|^2. \quad (42)$$

From the condition that the flagella initially grow if they start at zero length, we have $\pi_0 < 1$, and from the steady-state equation (20) it follows that $L_{ss} \leq 1/2$. Therefore

$$2\pi_0 J \pi_3 L_{ss} |\Delta L_1 - \Delta L_2|^2 < \pi_3 J |\Delta L_1 - \Delta L_2|^2. \quad (43)$$

It follows that $(\pi_3/2) |\Delta L_1 - \Delta L_2|^2 |\Delta L_1 + \Delta L_2|$ is bounded above by $\pi_3/\pi_1 \left(\pi_1 J (\Delta L_1 - \Delta L_2)^2 \right)$, where $\pi_1 J (\Delta L_1 - \Delta L_2)^2$ is the right-hand side of (29). Therefore,

$$\frac{d\phi}{dt} = \frac{1}{2} \left(\frac{d(\Delta L_1 + \Delta L_2)^2}{dt} + \frac{\pi_3}{\pi_1} \frac{d(\Delta L_1 - \Delta L_2)^2}{dt} \right) < 0. \quad (44)$$

□

Next, we consider whether Ω is a trapping region closed to the dynamics. That is, we must consider whether any trajectories originating in Ω may eventually leave Ω . First, we show that no trajectories cross the $L_1 + L_2 = 1$ boundary. To show that all trajectories move inward from this boundary, we calculate

$$\begin{aligned} \begin{pmatrix} L_1 \\ L_2 \end{pmatrix}' \Big|_{L_1+L_2=1} \cdot \begin{pmatrix} -1 \\ -1 \end{pmatrix} &= -(J(1-1) - \pi_0 - \pi_1 J L_1) - (J(1-1) - \pi_0 - \pi_1 J L_2) \\ &= 2\pi_0 + \pi_1 J (L_1 + L_2) > 0. \end{aligned} \quad (45)$$

This proves that trajectories flow inward cannot leave Ω across the $L_1 + L_2 = 1$ boundary. See Figure 3 for an illustration of Ω as well as the slope field and contours of $\phi(L_1, L_2)$.

In addition, for Ω to be a trapping region, no trajectories should escape the first quadrant. In terms of Ω , this means that no trajectories cross the L_1 axis on the interval $0 < L_1 \leq 1$, and no trajectories cross the L_2 axis on the interval $0 < L_2 \leq 1$. However, the model (8) and (9) does not satisfy this requirement. To the contrary,

$$\begin{pmatrix} L_1 \\ L_2 \end{pmatrix}' \Big|_{0 < L_1 \leq 1, L_2 = 0} \cdot \begin{pmatrix} 0 \\ 1 \end{pmatrix} = J(1 - L_1) - \pi_0, \quad (46)$$

and upon solving the quadratic equation resulting from $J(T - L_1) - \pi_0 = 0$ one finds that there is a unique positive root

$$L_{\text{crit}} = \frac{1 + \pi_0 \pi_2}{2\pi_0 \pi_3} \left(\sqrt{1 + \frac{4(1 - \pi_0) \pi_0 \pi_3}{(1 + \pi_0 \pi_2)^2}} - 1 \right). \quad (47)$$

Therefore, to prevent trajectories that cross the L_1 -axis resulting in unphysical negative lengths, we construct a hybrid system by setting $L_2' = 0$ when $L_1 > L_{\text{crit}}$ on $L_2 = 0$. This results in trajectories that flow down to the L_1 -axis, move horizontally according to this modified dynamics with $L_2' = 0$ until they reach $(L_1, L_2) = (L_{\text{crit}}, 0)$, at which point they rejoin the full dynamics and move toward steady state. The dynamics are modified symmetrically to prevent trajectories from crossing the L_2 -axis as well.

To characterize the trapping region of the full dynamics, we therefore define the trajectory $\omega_1(t)$ going backward in time from the point $(L_{\text{crit}}, 0)$, as defined by

$$\omega_1(0) = (L_{\text{crit}}, 0), \quad (48)$$

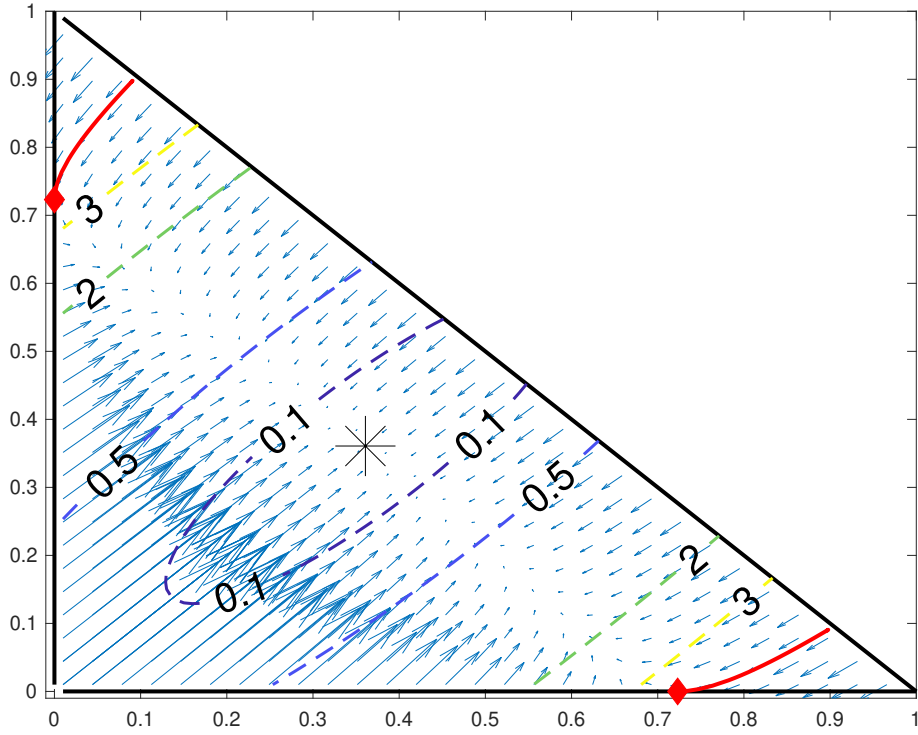


Figure 3: Dynamics of the active disassembly model. The slope field is plotted and contours $\phi(L_1, L_2) = C$ of the Lyapunov function $\phi(L_1, L_2)$ are shown for several values of C . The black asterisk denotes the unique steady state, the black curves represent boundaries of Ω , and the red diamonds represent the points $(L_{\text{crit}}, 0)$ and $(0, L_{\text{crit}})$ to which trajectories contract from the corner regions. The parameters used are $\pi_0 = 0.1$, $\pi_1 = 0.15$, $\pi_2 = 1$, and $\pi_3 = 2$.

up until it hits the diagonal $L_1 + L_2 = 1$. We define another trajectory $\omega_2(t)$ similarly as the one going backward in time from the point $(0, L_{\text{crit}})$. The points from which the trajectories $\omega_1(t)$ and $\omega_2(t)$ originate are illustrated by red diamonds and the trajectories are shown as red curves in Fig. 3.

As a consequence of the modified dynamics, trajectories originating in the corner regions of phase space bounded by $\omega_1(t)$ and $\omega_2(t)$ consist of three distinct phases: first, there is flow down to the L_1 or L_2 -axis, followed next by horizontal or vertical motion to the point $(L_{\text{crit}}, 0)$ or $(0, L_{\text{crit}})$, respectively, and finally leading to recovery by the full dynamics back to steady state. One interesting consequence of this behavior is its interpretation in the context of severing experiments. We find that the typical severing protocol, in which the two flagella first reach steady-state before severing takes place, does not lead to states within the corner region (purple trajectory in Fig. 4).

Fig. 4 shows a representative simulation of a severing experiment. The code used to generate this simulation and the corresponding figures is included in our public code repository located at <https://github.com/thomasgfai/StableFlagellarLengths>.

If the system is initially out of steady-state, however, severing may result in a state outside the trapping region. This yields two phases of flow after severing: first, a horizontal flow to the accumulation point L_{crit} , and second a flow by the full dynamics to reach the global steady-state (green trajectory in Fig. 4). As shown in the inset of Fig. 4(c), this first phase of horizontal flow leads to an apparent delay in the response of the cut flagellum.

One may reasonably ask the question of how a model derived based on a physical principles can lead to unphysical negative lengths. In this case, the origin of unphysical trajectories is the basal term d_0 in the disassembly model, which assumes there is a nonzero rate of disassembly even when the flagellum is very small. In the corner regions of the phase space, this basal term is greater than the rate of assembly and there is a negative growth rate at zero length because the long second flagellum leads to a tubulin pool that is nearly depleted. Note that this issue does not arise in agent-based models in which each tubulin monomer is represented explicitly, since in that case only assembly can occur when the flagellar length is zero. From this perspective, the modified dynamics essentially ensure that no more tubulin can be removed once there are no more tubulin monomers remaining on the flagellum.

2.1 Nonexistence of Oscillations: Alternate Proof

Recall that we have an invariant set on the domain Ω by construction. In this section, we use an alternative approach to exclude oscillations using standard methods in dynamical systems. The proof will primarily focus on the region of Ω containing the fixed point $(L_{\text{ss}}, L_{\text{ss}})$ that is bounded by the lines $L_2 = L_1 \pm \varepsilon$:

$$\Omega_\varepsilon := \{(L_1, L_2) \mid 0 \leq L_1, 0 \leq L_2, L_1 + L_2 \leq T, L_2 \leq L_1 + \varepsilon, L_1 - \varepsilon \leq L_2\},$$

where $0 < \varepsilon \leq L_{\text{crit}}$. An example of this domain is shown in Figure 5 for $\varepsilon = L_{\text{crit}}$ (checkerboard region). The boundary of Ω_ε for $\varepsilon = 0.2$ is shown using dotted lines, labeled

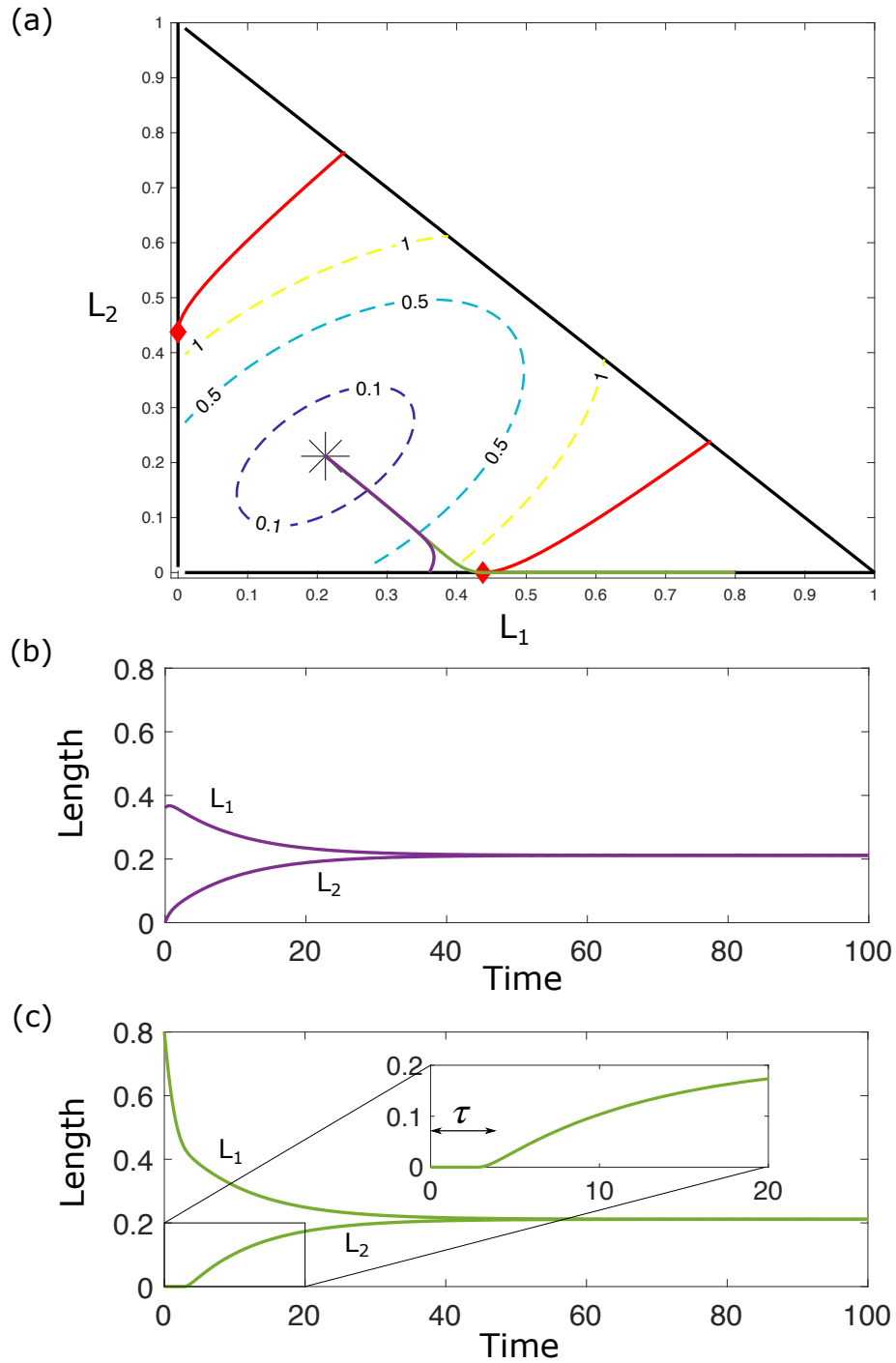


Figure 4: Upon severing, the pool size instantaneously decreases by the steady-state length L_{ss} . This leads to a rescaling of parameters. (a) A severing experiment is illustrated by plotting two trajectories in the L_1 - L_2 phase plane in green and purple, (b) and (c) Length vs. time corresponding respectively to the green and purple trajectories in (a). To allow for direct comparison to Fig. 3, the nondimensional parameters are obtained using the initial tubulin pool size prior to severing. The green trajectory is an example in which the flagella are initially equal at a value greater than the steady-state length. There is an initial delay τ as the longer flagellum shortens, during which the severed flagellum remains at zero length (see inset in (c)).

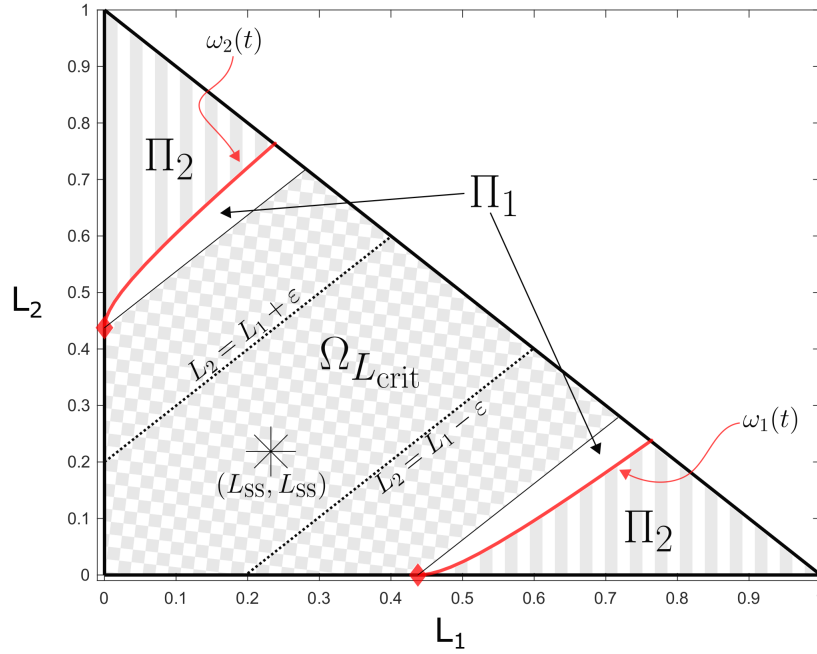


Figure 5: Domains of the alternative proof. $\Omega_{L_{\text{crit}}}$ (checkerboard region) denotes the region Ω_ε for $\varepsilon = L_{\text{crit}}$. Dotted lines show an example boundary of Ω_ε for $\varepsilon = 0.2$. Π_1 (white region) denotes the region between $\Omega_{L_{\text{crit}}}$ and the trajectories $\omega_1(t)$ and $\omega_2(t)$ (red curves). Π_2 (striped region) denotes the region outside of $\Omega_{L_{\text{crit}}}$ and π_1 but still inside the overall triangular domain Ω . The parameters are the same as in Figure 4.

$L_2 = L_1 \pm \varepsilon$. The smaller the value of ε , the thinner the domain Ω_ε will be. We will first show that Ω_ε is a trapping region (invariant set) for each ε arbitrarily small, by showing that the flows across the sections defined by the lines $L_2 = L_1 \pm \varepsilon$ are always inward towards the fixed point L_{SS} . This condition is sufficient because we have already shown that flow along the relevant boundaries of Ω point inwards, specifically, $(L_1, 0)$ and $(0, L_2)$ for $L_1, L_2 \in [0, L_{\text{crit}}]$, and $L_1 + L_2 = 1$. To prove the non-existence of oscillations, we assume it exists and show that a portion of the oscillation must escape Ω_ε for some ε and can not return, which is a contradiction.

Claim. Ω_ε is an invariant set.

In the ensuing proof, we show that the flows across the sections defined by the lines $L_2 = L_1 \pm \varepsilon$ are always inward towards the fixed point L_{SS} . Combined with the inward flow along the boundaries of Ω , this inward flow across the lines $L_2 = L_1 \pm \varepsilon$ is sufficient to prove the claim.

Proof. To show that the vector field points inwards for a given Ω_ε , we show that $dL_1/dt > dL_2/dt$ along $L_2 = L_1 + \varepsilon$ and $dL_1/dt < dL_2/dt$ along $L_2 = L_1 - \varepsilon$. First, we plug in

$L_2 = L_1 + \varepsilon$ into the right hand side of (8) and (9) and take the difference $dL_1/dt - dL_2/dt$:

$$\begin{aligned}\frac{dL_1}{dt} - \frac{dL_2}{dt} &= J(1 - L_1 - L_2) - \pi_0 - \pi_1 J L_1 - [J(1 - L_1 - L_2) - \pi_0 - \pi_1 J L_2] \\ &= -\pi_1 J L_1 + \pi_1 J (L_1 + \varepsilon) \\ &= \pi_1 J \varepsilon > 0.\end{aligned}$$

Therefore, $dL_1/dt > dL_2/dt$ independent of the choice of ε . Inward flow along the lower boundary follows using the same argument. Thus, for each ε , the set Ω_ε is invariant.

We now proceed with a proof by contradiction. Suppose that there exists a periodic solution. Every oscillating solution must surround at least one fixed point (see index theory, [19]), and the only fixed point of this system exists within Ω_ε . Therefore, the oscillating solution surrounds the fixed point (L_{ss}, L_{ss}) , and there exists some ε^* such that parts of the periodic solution lie outside of Ω_{ε^*} . (If an oscillating solution is fully contained within Ω_ε for some ε , to obtain ε^* we may simply reduce ε until parts of the periodic solution lie outside of Ω_{ε^*} .) It follows that solutions must exit Ω_{ε^*} , but this contradicts Ω_{ε^*} being an invariant set. \square

2.2 Global Asymptotic Stability: Alternate Proof

Claim. *The fixed point (L_{ss}, L_{ss}) is globally asymptotically stable in Ω .*

Proof. We will consider three parts of the domain. First, $\Omega_{L_{crit}} := \Omega_\varepsilon$ for $\varepsilon = L_{crit}$ (Figure 5, checkerboard region), second, the region between $\Omega_{L_{crit}}$ and ω_1 which we call Π_1 (Figure 5, white region within Ω), and third, the region $\Pi_2 := \Omega \setminus (\Omega_{L_{crit}} \cup \Pi_1)$ (Figure 5, striped region). The sets $\Omega_{L_{crit}}$, Π_1 , and Π_2 are taken to be closed.

We begin our proof with Π_1 and Π_2 because they are the most straightforward. In Π_1 , all solutions exit through one of the lines $L_2 = L_1 \pm L_{crit}$. This observation follows because there are no fixed points in Π_1 and flows cannot cross the solution ω_1 . In Π_2 , we force all flows to exit through $(L_{crit}, 0)$ or $(0, L_{crit})$ by definition. Therefore, all flows originating in $\Pi_1 \cup \Pi_2$ will enter the trapping region $\Omega_{L_{crit}}$.

It remains to show asymptotic stability in $\Omega_{L_{crit}}$. Note that our system is continuously differentiable on all of $\Omega_{L_{crit}}$ and therefore existence and uniqueness of solutions holds for all time. Before proceeding with the proof of asymptotic stability, we recall two basic definitions.

Definition 1. *The **positive semiorbit** is defined as the set*

$$\gamma(\mathbf{p}) = \{\mathbf{x} \in \mathbb{R}^2 : \mathbf{x} = \phi(t, \mathbf{p}), \text{ for some } t \in (0, \infty)\}.$$

Definition 2. *The **ω -limit set** of a point $\mathbf{x} \in M$, $\omega(\mathbf{x})$, is the set of those points $\mathbf{y} \in M$ for which there exists a sequence $t_n \rightarrow \infty$ with $\phi(t_n, \mathbf{x}) \rightarrow \mathbf{y}$, where ϕ is the flow of an autonomous ODE $\dot{\mathbf{x}} = F(\mathbf{x})$, and M is an open subset of \mathbb{R}^2 [20]. The **omega-limit set** $\omega(\gamma)$ for a trajectory γ is defined analogously.*

In the case that all solutions are bounded, only certain types of ω -limit sets are possible. This is a consequence of the following theorem (Theorem 7.4.2 in [21]):

Theorem 1. *Let γ be a positive semiorbit contained in a compact subset K of \mathbb{R}^2 and suppose that K contains only a finite number of equilibrium points. Then*

1. $\omega(\gamma)$ consists of a single point \mathbf{p} which is an equilibrium point of \mathbf{F} , and for an initial condition $\mathbf{x}(0) \in \gamma$, $\mathbf{x}(t) \rightarrow \mathbf{p}$ as $t \rightarrow \infty$, or
2. $\omega(\gamma)$ is a periodic orbit, or
3. $\omega(\gamma)$ consists of a finite set of equilibrium points together with their connecting orbits. Each such orbit approaches an equilibrium point on $t \rightarrow \infty$ and as $t \rightarrow -\infty$.

This theorem, which follows from the Poincaré-Bendixson theorem, tells us that if a solution is trapped in a compact domain for all time, then a single equilibrium must be either a unique asymptotically stable point or a saddle-like point with at least one pair of connected unstable and stable manifolds. (The saddle-like observation follows by the third part of the theorem; a single equilibrium can also be stable in backwards time.)

Because we have eliminated periodic orbits in $\Omega_{L_{\text{crit}}}$ and shown that our stable fixed point $(L_{\text{ss}}, L_{\text{ss}})$ is locally asymptotically stable and therefore cannot be saddle-like, we must have an asymptotically stable equilibrium point in $\Omega_{L_{\text{crit}}}$. Finally, because all solutions in $\Omega \setminus \Omega_{L_{\text{crit}}}$ eventually reach the trapping region $\Omega_{L_{\text{crit}}}$, $(L_{\text{ss}}, L_{\text{ss}})$ is the globally asymptotically stable equilibrium point in Ω . \square

2.3 Generalization to organisms with $N > 2$ flagella

Here we generalize the Lyapunov function to arbitrary N . In this case, the equations corresponding to (5) to (7) are:

$$\frac{dL_i}{dt} = \gamma J \left(T - \sum_{j=1}^N L_j \right) - d_0 - d_1 \frac{JL_i}{D}, \quad i = 1, \dots, N, \quad (49)$$

$$J(L_1, \dots, L_N) = \frac{k_{\text{on}} M / N}{1 + (k_{\text{on}} / Nv) \sum_{j=1}^N L_j + (k_{\text{on}} / 2ND) \sum_{j=1}^N L_j^2}. \quad (50)$$

To put the equations in dimensionless form, we follow the approach taken in the case $N = 2$ above by introducing the dimensionless variables $\tilde{L}_i = L_i / T$ and $\tilde{t} = t \gamma k_{\text{on}} M / N$ as well as the dimensionless parameters $\pi_0 = Nd_0 / \gamma k_{\text{on}} MT$, $\pi_1 = d_1 / \gamma D$, $\pi_2 = k_{\text{on}} T / Nv$, and $\pi_3 = k_{\text{on}} T^2 / ND$. This leads to the following system, which generalizes (8) to (10) above:

$$\frac{d\tilde{L}_i}{d\tilde{t}} = \tilde{J} \left(1 - \sum_{j=1}^N \tilde{L}_j \right) - \pi_0 - \pi_1 \tilde{J} \tilde{L}_i, \quad i = 1, \dots, N, \quad (51)$$

$$\tilde{J} = \frac{1}{1 + \pi_2 \sum_{j=1}^N \tilde{L}_j + \pi_3 \sum_{j=1}^N \tilde{L}_j^2}. \quad (52)$$

As in the case $N = 2$, (51) leads to a unique fixed point with $\tilde{L}_i = \tilde{L}_{ss}$ for $i = 1, \dots, N$ with

$$\tilde{L}_{ss} = \frac{1 + \pi_0\pi_2 + \pi_1/N}{2\pi_0\pi_3} \left(\sqrt{1 + \frac{4(1 - \pi_0)\pi_0\pi_3}{N(1 + \pi_0\pi_2 + \pi_1/N)^2}} - 1 \right), \quad (53)$$

which decays as $1/N$ as $N \rightarrow 0$.

Note that, in the limit $N \rightarrow \infty$ for fixed T and M , the dimensionless basal disassembly parameter π_0 satisfies $\pi_0 \rightarrow \infty$. This is because the injection rate into any one flagellum, which goes as $1/N$, becomes smaller and smaller in comparison to the N -independent basal disassembly d_0 , resulting in steady-state lengths of zero beyond a critical value of N . However, in the special case $d_0 = 0$, one obtains flagella of progressively smaller but nonzero lengths as $N \rightarrow 0$.

Next, we prove global asymptotic stability by constructing a Lyapunov function, following similar logic to that used in the $N = 2$ case. In the following, we once again drop the tildes for convenience. Define $\Delta L_i = L_i - L_{ss}$ as before for $i = 1, \dots, N$ and let

$$\phi(L_1, \dots, L_N) = \frac{1}{2} \left[\left(\sum_{i=1}^N \Delta L_i \right)^2 + \frac{2\pi_3}{\pi_1} \sum_{i \neq j} (\Delta L_i - \Delta L_j)^2 \right]. \quad (54)$$

Claim. ϕ is a Lyapunov function on Ω .

Proof. We first note that setting the derivative to zero in (51) yields the identify

$$0 = J_{ss} (1 - NL_{ss}) - \pi_0 - \pi_1 J_{ss} L_{ss}. \quad (55)$$

where

$$J_{ss} = \frac{1}{1 + N\pi_2 L_{ss} + N\pi_3 L_{ss}^2}. \quad (56)$$

Following the logic of the proof in the case $N = 2$ results in the equations

$$\frac{1}{2} \frac{d}{dt} \left(\sum_{i=1}^N \Delta L_i \right)^2 = N(J - J_{ss})(1 - NL_{ss} - \pi_1 L_{ss}) \sum_{i=1}^N \Delta L_i - (N + \pi_1) J \left(\sum_{i=1}^N \Delta L_i \right)^2 \quad (57)$$

$$\frac{1}{2} \frac{d}{dt} (\Delta L_i - \Delta L_j)^2 = -\pi_1 J (\Delta L_i - \Delta L_j)^2, \quad \text{for } i \neq j. \quad (58)$$

From the steady-state identify (55), we have

$$1 - NL_{ss} - \pi_1 L_{ss} = \frac{\pi_0}{J_{ss}}, \quad (59)$$

so that the first term on the right-hand side of (57) may be rewritten as

$$\begin{aligned} N(J - J_{ss})(1 - NL_{ss} - \pi_1 L_{ss}) \sum_{i=1}^N \Delta L_i &= \frac{N\pi_0}{J_{ss}} (J - J_{ss}) \sum_{i=1}^N \Delta L_i \\ &= N\pi_0 J (J_{ss}^{-1} - J^{-1}) \sum_{i=1}^N \Delta L_i. \end{aligned} \quad (60)$$

The expression above may be simplified further by using the definition of the flux to obtain

$$J_{ss}^{-1} - J^{-1} = -\pi_2 \sum_{i=1}^N \Delta L_i - \pi_3 \sum_{i=1}^N (L_i^2 - L_{ss}^2), \quad (61)$$

and noting that

$$\begin{aligned} \sum_{i=1}^N (L_i^2 - L_{ss}^2) &= \sum_{i=1}^N (L_i + L_{ss}) \Delta L_i \\ &= \sum_{i=1}^N L_i \Delta L_i + L_{ss} \sum_{i=1}^N \Delta L_i. \end{aligned} \quad (62)$$

Moreover, we may rewrite the first term on the right-hand side above by adding and subtracting $(\frac{1}{N} \sum_{i=1}^N L_i) \sum_{i=1}^N \Delta L_i$ to obtain

$$\begin{aligned} \sum_{i=1}^N L_i \Delta L_i &= \left(\frac{1}{N} \sum_{i=1}^N L_i \right) \sum_{i=1}^N \Delta L_i + \sum_{i=1}^N \left(L_i - \frac{1}{N} \sum_{i=1}^N L_i \right) \Delta L_i \\ &= \left(\frac{1}{N} \sum_{i=1}^N L_i \right) \sum_{i=1}^N \Delta L_i + \frac{1}{N} \sum_{i=1}^N \left(\sum_{j \neq i} \Delta L_i - \Delta L_j \right) \Delta L_i. \end{aligned} \quad (63)$$

Combining (60) to (63) yields

$$\begin{aligned} N\pi_0 J (J_{ss}^{-1} - J^{-1}) \sum_{i=1}^N \Delta L_i &= -N\pi_0 J \left(\pi_2 \left(\sum_{i=1}^N \Delta L_i \right)^2 + \pi_3 L_{ss} \left(\sum_{i=1}^N \Delta L_i \right)^2 \right. \\ &\quad \left. + \frac{\pi_3}{N} \left(\sum_{i=1}^N L_i \right) \left(\sum_{i=1}^N \Delta L_i \right)^2 + \frac{\pi_3}{N} \left(\sum_{i=1}^N \Delta L_i \right) \sum_{i \neq j} (\Delta L_i - \Delta L_j)^2 \right). \end{aligned} \quad (64)$$

The first three terms in parentheses on the right-hand side of (64) are clearly positive. The final term may be bounded according to

$$\left| \frac{\pi_3}{N} \left(\sum_{i=1}^N \Delta L_i \right) \sum_{i \neq j} (\Delta L_i - \Delta L_j)^2 \right| \leq \frac{\pi_3}{N} \left| \sum_{i=1}^N \Delta L_i \right| \left| \sum_{i \neq j} (\Delta L_i - \Delta L_j)^2 \right| \leq \frac{2\pi_3}{N} \sum_{i \neq j} (\Delta L_i - \Delta L_j)^2, \quad (65)$$

where the final inequality follows from $\left| \sum_{i=1}^N \Delta L_i \right| \leq \left| \sum_{i=1}^N L_i \right| + \left| \sum_{i=1}^N L_{ss} \right| \leq 2$, by (55) and the definition of Ω , which asserts that the sum of lengths must not exceed the total pool.

Therefore, substituting (64) and (65) into (57) and (58) results in

$$\begin{aligned} \frac{d\phi}{dt} &\leq 2\pi_3 \sum_{i \neq j} (\Delta L_i - \Delta L_j)^2 - \frac{2\pi_3}{\pi_1} \sum_{i \neq j} \left(\pi_1 J (\Delta L_i - \Delta L_j)^2 \right) \\ &\leq 2\pi_3 \sum_{i \neq j} (\Delta L_i - \Delta L_j)^2 - 2\pi_3 \sum_{i \neq j} (\Delta L_i - \Delta L_j)^2 \leq 0, \end{aligned} \quad (66)$$

with equality obtained at the unique steady-state, i.e. ϕ satisfies the requirement of a Lyapunov function. \square

Note that the Lyapunov function we construct for general N does not reduce to the Lyapunov function constructed previously in the case $N = 2$. There is an additional factor of two in the second term of ϕ . However, there is no inconsistency; the Lyapunov function is not unique. Still, the Lyapunov function constructed previously provides a tighter bound in the case $N = 2$, and we conjecture that the factor of two in the second term of the Lyapunov function in (54) is not essential.

3 Discussion

We have studied the properties of the dynamical system proposed as an active disassembly model of flagellar length control proposed in [13]. We have described the region of validity for the model and used the method of Lyapunov function as well as the Poincare-Bendixson to prove the existence of an asymptotically stable steady-state. Although the Poincare-Bendixson method is limited to systems of two equations, the Lyapunov approach is shown to generalize to $N > 2$.

Interestingly, we find that the phase space of physically-allowable lengths is not a trapping region with respect to the dynamics. Therefore, we must modify the dynamics in the corner regions from which trajectories are carried outside the first quadrant. This results in two accumulation points; however, we show that the unique dynamics associated with these accumulation points are not likely to arise in application.

The generality of the approach taken here remains an open question. The proofs given here are independent of the model parameters. However, if the model were perturbed slightly to involve additional terms, it is not clear whether the same Lyapunov function approach would still apply. Characterizing the family of models for which this approach succeeds would be a valuable step toward establishing the mathematical properties of balance-point models more generally.

A related open question is whether there exists an optimal Lyapunov function in the sense of providing the tightest possible bound, and if so, whether this may provide biological intuition into the energetics of length control.

Finally, we discuss aspects of length control in the case of a large number of organelles. Indeed, this is a biologically-relevant case given that single-cell organisms such as *Paramecium* cells swim using on the order of five thousand cilia. Depending on which parameters are fixed in the limit $N \rightarrow \infty$, our dimensional analysis of the active disassembly model yields different limiting behaviors. A remarkable consequence of the model is that it provides a universal length-control mechanism regardless of organelle number, and an important next step would be to establish the limits of the model by testing its predictions on different organisms over a range of N .

4 Acknowledgments

We thank Ariel Amir and Te Cao for providing feedback on an early version of this manuscript. We acknowledge useful discussions with Prathitha Kar, Lishibanya Mohapatra, and Jane Kondev. We acknowledge support under National Science Foundation grant DMS-1913093 (TGF) and National Institute of Health grant T32 NS007292 (YP).

References

- [1] D. Zink, A. H. Fischer, J. A. Nickerson, Nuclear structure in cancer cells, *Nature Reviews Cancer* 4 (9) (2004) 677–687.
- [2] J. B. S. Haldane, On being the right size, *Harper’s Magazine* 152 (1926) 424–427.
- [3] W. F. Marshall, Cell geometry: How cells count and measure size, *Annual Review of Biophysics* 45 (2016) 49–64.
- [4] R. Milo, R. Phillips, *Cell biology by the numbers*, Garland Science, 2015.
- [5] K. A. Wemmer, W. F. Marshall, Flagellar length control in chlamydomonas—a paradigm for organelle size regulation, *International review of cytology* 260 (2007) 175–212.
- [6] B. L. Gutman, K. K. Niyogi, Chlamydomonas and arabidopsis. a dynamic duo, *Plant Physiology* 135 (2) (2004) 607–610.
- [7] R. E. Goldstein, Green algae as model organisms for biological fluid dynamics, *Annual review of fluid mechanics* 47 (2015) 343–375.
- [8] P. A. Salomé, S. S. Merchant, A series of fortunate events: Introducing chlamydomonas as a reference organism, *The Plant Cell* 31 (8) (2019) 1682–1707.
- [9] K. Y. Wan, G. Jékely, On the unity and diversity of cilia (2020).

- [10] R. L. Nguyen, L.-W. Tam, P. A. Lefebvre, The *lf1* gene of *chlamydomonas reinhardtii* encodes a novel protein required for flagellar length control, *Genetics* 169 (3) (2005) 1415–1424.
- [11] D. K. Khona, V. G. Rao, M. J. Motiwalla, P. S. Varma, A. R. Kashyap, K. Das, S. M. Shirolkar, L. Borde, J. A. Dharmadhikari, A. K. Dharmadhikari, et al., Anomalies in the motion dynamics of long-flagella mutants of *chlamydomonas reinhardtii*, *Journal of biological physics* 39 (1) (2013) 1–14.
- [12] J. L. Rosenbaum, J. E. Moulder, D. L. Ringo, Flagellar elongation and shortening in *chlamydomonas*: the use of cycloheximide and colchicine to study the synthesis and assembly of flagellar proteins, *The Journal of Cell Biology* 41 (2) (1969) 600–619.
- [13] T. G. Fai, L. Mohapatra, P. Kar, J. Kondev, A. Amir, Length regulation of multiple flagella that self-assemble from a shared pool of components, *Elife* 8 (2019) e42599.
- [14] W. F. Marshall, J. L. Rosenbaum, Intraflagellar transport balances continuous turnover of outer doublet microtubules implications for flagellar length control, *The Journal of cell biology* 155 (3) (2001) 405–414.
- [15] W. F. Marshall, H. Qin, M. R. Brenni, J. L. Rosenbaum, Flagellar length control system: testing a simple model based on intraflagellar transport and turnover, *Molecular biology of the cell* 16 (1) (2005) 270–278.
- [16] K. G. Kozminksi, K. A. Johnson, P. Forscher, J. L. Rosenbaum, A motility in the eukaryotic flagellum unrelated to flagellar beating, *Proceedings of the National Academy of Sciences* 90 (12) (1993) 5519–5523.
- [17] A. Chien, S. M. Shih, R. Bower, D. Tritschler, M. E. Porter, A. Yildiz, Dynamics of the ift machinery at the ciliary tip, *Elife* 6 (2017) e28606.
- [18] N. L. Hendel, M. Thomson, W. F. Marshall, Diffusion as a ruler: modeling kinesin diffusion as a length sensor for intraflagellar transport, *Biophysical journal* 114 (3) (2018) 663–674.
- [19] J. Guckenheimer, P. Holmes, Local bifurcations, in: *Nonlinear oscillations, dynamical systems, and bifurcations of vector fields*, Springer, 1983, pp. 117–165.
- [20] G. Teschl, *Ordinary differential equations and dynamical systems*, Vol. 140, American Mathematical Soc., 2012.
- [21] N. Lebovitz, *Ordinary differential equations*, Cengage Learning, 2019.